Journal of Experimental Botany, Vol. 75, No. 16 pp. 4760–4771, 2024
https://doi.org/10.1093/jxb/erae243 Advance Access Publication 23 May 2024

TECHNICAL INNOVATION

Biolistics-mediated transformation of hornworts and its application to study pyrenoid protein localization

Declan J. Lafferty[1], Tanner A. Robison[1,2], Andika Gunadi[3], Peter W. Schafran[1], Laura H. Gunn[2,4], Joyce Van Eck[1,5], and Fay-Wei Li[1,2,*]

[1] Boyce Thompson Institute, Ithaca, NY 14853, USA
[2] Plant Biology Section, School of Integrative Plant Science, Cornell University, Ithaca, NY 14853, USA
[3] J.R. Simplot Company, Boise, ID 83707, USA
[4] Plant Department of Cell and Molecular Biology, Uppsala University, S-751 24 Uppsala, Sweden
[5] Plant Breeding and Genetics Section, School of Integrative Plant Science, Cornell University, Ithaca, NY 14853, USA

* Correspondence: fl329@cornell.edu

Received 23 October 2023; Editorial decision 15 May 2024; Accepted 22 May 2024

Editor: John Lunn, MPI of Molecular Plant Physiology, Germany

Abstract

Hornworts are a deeply diverged lineage of bryophytes and a sister lineage to mosses and liverworts. Hornworts have an array of unique features that can be leveraged to illuminate not only the early evolution of land plants, but also alternative paths for nitrogen and carbon assimilation via cyanobacterial symbiosis and a pyrenoid-based CO_2-concentrating mechanism (CCM), respectively. Despite this, hornworts are one of the few plant lineages with limited available genetic tools. Here we report an efficient biolistics method for generating transient expression and stable transgenic lines in the model hornwort, *Anthoceros agrestis*. An average of 569 (±268) cells showed transient expression per bombardment, with green fluorescent protein expression observed within 48–72 h. A total of 81 stably transformed lines were recovered across three separate experiments, averaging six lines per bombardment. We followed the same method to transiently transform nine additional hornwort species, and obtained stable transformants from one. This method was further used to verify the localization of Rubisco and Rubisco activase in pyrenoids, which are central proteins for CCM function. Together, our biolistics approach offers key advantages over existing methods as it enables rapid transient expression and can be applied to widely diverse hornwort species.

Keywords: *Anthoceros agrestis*, biolistics, bryophyte, CO_2-concentrating mechanism, fluorescent protein tagging, gene gun, hornwort, pyrenoid.

Introduction

Hornworts are a unique group of bryophytes that exhibit distinct traits among land plants. Evolutionarily, hornworts diverged from the closest extant clade, setaphytes (mosses and liverworts), over 480 million years ago (Morris *et al.*, 2018). Many of hornworts' developmental, anatomical, and physiological features are not found in other plant lineages. As such, hornworts are of paramount importance in retracing plant evolutionary history (Li *et al.*, 2020; Frangedakis *et al.*, 2021a).

Abbreviations: BUSCO, Benchmarking Universal Single-Copy Orthologue; CCM, CO_2-concentrating mechanism; CDS, coding sequence; Ef1α, elongation factor 1α; GFP, green fluorescent protein; HPT, hygromycin phosphorylase; RbcS, Rubisco small subunit; RCA, Rubisco activase; Rubisco, ribulose-1,5-bisphosphate carboxylase/oxygenase.

Hornworts have evolved unconventional ways to source nitrogen and carbon. For nitrogen, all hornwort species are known to engage in a symbiotic relationship with nitrogen-fixing cyanobacteria (Meeks, 1998; Nelson *et al.*, 2021). Symbiotic cyanobacteria are hosted inside specialized slime cavities in the hornwort thallus, where they differentiate into heterocysts, a cell type dedicated to nitrogen fixation. While several hornwort genes have been recently identified that might be involved in symbiosis regulation or maintenance (Li *et al.*, 2020; Chatterjee *et al.*, 2022), they have not been functionally characterized.

For carbon capture, hornworts are the only land plants that evolved a pyrenoid-based CO_2-concentrating mechanism (CCM). In this case, the CO_2-fixing enzyme, ribulose-1,5-bisphosphate carboxylase/oxygenase (Rubisco), is compartmentalized inside pyrenoids, which are special chloroplast structures sandwiched by thylakoids (Vaughn *et al.*, 1992). Through the coordinated actions of bicarbonate transporters and carbonic anhydrases, CO_2 is concentrated within pyrenoids thereby boosting the efficiency of Rubisco (Li *et al.*, 2017; He *et al.*, 2023). Interestingly, pyrenoids (and the associated CCM) have been repeatedly gained and lost during hornwort evolution (Villarreal and Renner, 2012), providing unique evolutionary replications for examining the underlying genetic mechanisms. It has been hypothesized that engineering a biophysical CCM into crop plants could enhance photosynthetic efficiency (Adler *et al.*, 2022), but attempts to transfer algal pyrenoid-based CCMs are challenged by the incompatibility between land plant Rubisco and algal pyrenoid components (Meyer *et al.*, 2016; Atkinson *et al.*, 2020). On the other hand, hornwort Rubisco and chloroplasts are both evolutionarily and structurally similar to those in crop plants, providing a CCM that may be more readily engineered into crops. Currently, none of the genetic components of hornwort pyrenoid structure and development have been identified, outside of Rubisco.

Anthoceros agrestis has recently emerged as a potential model hornwort species, with a sequenced genome and an optimized tissue culture growth medium (Szövényi *et al.*, 2015; Li *et al.*, 2020; Gunadi *et al.*, 2022). Its life cycle is dominated by a haploid gametophyte stage, making it an ideal target for genetic engineering. However, the lack of transformation tools has hampered the progress of functional genomics in hornworts. Recently, an *Agrobacterium*-mediated transformation method was reported for *A. agrestis* and has been successfully used for a number of hornwort species (Frangedakis *et al.*, 2021b; Waller *et al.*, 2023). Transient transformation of hornwort protoplasts has also been reported (Neubauer *et al.*, 2022), although thallus regeneration from protoplasts has not been possible. The biolistic method, also known as particle bombardment or gene gun technology, is another powerful tool used for genetic engineering (Sanford *et al.*, 1987) and has not been explored for hornworts. This method involves the introduction of microscopic particles coated with DNA into plant cells.

Biolistics has a number of advantages over other transformation methods. First, it is relatively simple and requires less technical expertise. The preparation time for biolistics is relatively fast, taking less than a couple of hours for particle preparation and subsequent transformation. *Agrobacterium*-mediated methods involve the use of live bacteria and co-cultivation steps, and protoplast transformation requires cell wall digestion, all of which can be difficult to optimize (Lacroix and Citovsky, 2020). Second, biolistics can deliver a wider range of cargoes into plant cells including plasmid DNA, linearized DNA (such as PCR products), RNA, ribonucleoproteins, and proteins (Fu *et al.*, 2000; Martin-Ortigosa and Wang, 2014; Svitashev *et al.*, 2016; Zhang *et al.*, 2016). Finally, biolistics can be used to transform plastids (Boynton *et al.*, 1988; Svab and Maliga, 1993), which is crucial to study the genes involved in pyrenoid function. Conversely, the downsides of the biolistic method include the possibility of causing severe cellular damage and the method may require expensive supplies and equipment. Reports have also shown a higher number of integrated gene copies when compared with *Agrobacterium*-mediated transformation, potentially causing genetic instability and gene silencing (Kohli *et al.*, 2003). The extent of these impacts, however, has not yet been explored in hornworts.

In this study, we describe the development of a biolistic transformation method for hornworts, demonstrating both transient and stable transformation of *A. agrestis* and *Anthoceros fusiformis*, as well as transient transformation of nine other species across the hornwort tree of life. These transformable species share the most recent common ancestor almost 300 million years ago, before the origin of flowering plants. Using our optimized method, we were able to observe transient expression of the green fluorescent protein (GFP) reporter gene within 48–72 h of transformation, and recover stable transgenic lines after 8–10 weeks. Importantly, we applied this method to examine the subcellular localization of Rubisco and Rubisco activase, both of which are key elements in CCMs. Together, our study provides a new tool for comparative research across bryophytes and vascular plants.

Materials and methods

Plant tissue preparation

Hornwort cultures were grown axenically on AG medium supplemented with 0.2% sucrose at 22 °C under a 16/8 h light/dark cycle with 6–25 μmol m^{-2} s^{-1} light intensity provided by Ecolux XL Starcoat F32T8 XL SP30 ECO paired with F32T8 XL SP41 ECO fluorescence bulbs (General Electric, USA) as described in Gunadi *et al.* (2022). One litre of AG medium consists of 100 ml Hatcher's stock A, 3 ml Hatcher's stock B, 1 ml Hatcher's stock C (Hatcher, 1965), 0.2% or 2% sucrose, 5 mM MES (pH 6.5 with KOH) (M5287, Sigma-Aldrich, USA), 4 g gelzan (G3251, PhytoTech Labs, USA), 100 mg activated charcoal (C-3345, Sigma-Aldrich), 1 mg ml^{-1} 6-benzylaminopurine (B3408, Merck, Germany), and 300 mg l^{-1} timentin (T-104-25, Goldbio, USA). Thallus tissue (haploid) was prepared for transformation by placing 3–6 g (fresh weight) of tissue in a 50 ml Falcon tube containing 30 ml of sterile deionized water supplemented with 30 μl of 300 mg ml^{-1} timentin (final concentration

of 300 mg l^{-1}), followed by homogenization with a T18 digital ULTRA TURRAX homogenizer (IKA, Germany) for 5 s at 4000 rpm. The tissue was filtered using a 100 µM cell strainer (C4100, MTC Bio, USA) and washed with 50 ml sterile deionized water. Approximately 200 mg of tissue was plated on AG medium, supplemented with 2% sucrose. Tissue was spread as thinly as possible in a 2.5 cm circle using a Nunc cell scraper (Thermo Fisher Scientific, USA). The plates were left open for 10 min to remove excess moisture. Tissue was allowed to recover for 7 d before transformation. These procedures were done in a laminar flow hood. All hornwort species used in this study were subjected to the same growth conditions.

DNA construct preparation

Constructs were designed using the OpenPlant toolkit (Sauret-Güeto *et al.*, 2020). The Aa049 construct (Supplementary Fig. S1) was assembled using the following L0 parts: native *A. agrestis Elongation factor 1 alpha* (*Ef1α*) promoter, OP_049 35S promoter, OP-020 *hygromycin phosphotransferase* (*hpt*), OP_023 *eGFP*, OP_037 *CTAG_Lti6b*, and OP_053 *NoS* terminator. Vector ligations and *Escherichia coli* transformation were performed as described in Frangedakis *et al.* (2021b). To obtain high concentrations of plasmid DNA, 100 ml of *E. coli* culture was grown overnight at 37 °C. The plasmid DNA was extracted using the PureYield Plasmid Midiprep System (A2492, Promega, USA), followed by vacuum concentration in a SpeedVac Concentrator (Thermo Fisher Scientific) to obtain DNA concentrations of 1 µg $µl^{-1}$.

Gold particle preparation

To prepare for 10 separate bombardments, a total of 20 µl of 1 µg $µl^{-1}$ plasmid DNA was combined with 50 µl of gold microparticles (1 µm, 50 mg ml^{-1}, suspended in 50% (v/v) sterile glycerol) (1652263, Bio-Rad Laboratories, USA), 100 µl of 2.5 M $CaCl_2$, and 40 µl of 0.1 M spermidine (S0266, Sigma-Aldrich), under constant vortexing. The DNA/gold mixture was vortexed for 1 min before being pelleted by centrifugation at 3500×*g* for 8 s. The supernatant was removed and 180 µl of 70% (v/v) ethanol was added and vortexed for 1 min. The DNA/gold mixture was centrifuged again at 3500×*g* for 8 s. The supernatant was removed and 200 µl of 100% ethanol was added and vortexed for 1 min, followed by another centrifugation step and the removal of 135 µl of supernatant. The DNA/gold mixture was resuspended in a Branson 2510 Ultrasonic Cleaner and 5 µl was spread onto each sterilized macrocarrier (1652335, Bio-Rad) and left to dry for 30 min.

Biolistic transformation

Biolistics was performed using the Particle Delivery System PDS-1000/He (1652257, Bio-Rad). Thallus tissue was bombarded with a target distance of 14 cm, under a vacuum of 711 mmHg. The burst pressure was generated using a 450 psi rupture disk (1652326, Bio-Rad). The macrocarrier and rupture disc were retained using a stopping screen (1652257, Bio-Rad). The tissue was left to recover for 7 d. In this study, a total of five separate experiments were conducted, each with 10 replicate plates, to assess the transient transformation efficiency and consistency.

Imaging and quantification of transient transformation efficiency

Transient transformation efficiency was estimated using a pipeline developed in CellProfiler (v4.2.5) (Stirling *et al.*, 2021). Fluorescent images of transformed tissues were taken 48–72 h post bombardment, using a GFP filter on a Leica M205 stereomicroscope. Nine images, each with a dimension of 10 mm×7.5 mm, were taken to encompass all tissue used for transformation. The exposure time was set between 10 and 12 s, depending on transient GFP fluorescent intensity, and was kept constant for all images within an experiment. The default pipeline parameters were used with adjustments made to cell diameter (between 6 and 30 pixel units in diameter) and object intensity (green intensity between 0.1 and 0.9). Red signals represent cells expressing GFP and blue signals are objects classified by CellProfiler that are not expressing GFP; these may be artifacts or untransformed cells/tissue. The pipeline can be found on Figshare (http://doi.org/10.6084/m9.figshare.24243559). The number of transients in each image were combined to show the total transients in each replicate.

Regeneration of stably transformed lines

To regenerate stably transformed lines, tissue from all successfully transformed replicate plates was pooled and homogenized (as described above) 7 d post-bombardment. The homogenized tissues were collected using a 100 µm cell strainer, washed with sterile water, and thinly spread on 70 mm diameter Whatman filter paper (WHA1001070, Sigma-Aldrich) overlain on solid AG medium supplemented with 0.2% sucrose. The number of plates prepared corresponds to the number of replicates pooled. The tissue was left to recover for 3 d before transfer to AG medium supplemented with 0.2% sucrose and 10 mg l^{-1} hygromycin (10687010, Thermo Fisher Scientific) by moving the filter paper containing the tissue. After 4 weeks the tissue was transferred to freshly prepared AG medium supplemented with 0.2% sucrose and 10 mg l^{-1} hygromycin. Stably transformed thallus tissue is visible within 8–10 weeks of transformation (Fig. 1). Images were taken on a Leica M205 stereomicroscope and a Leica TCS SP5 laser scanning confocal microscope. Figure 1 displays an overview of the biolistics transformation protocol.

Transgene confirmation by PCR

Presence of the transgene was confirmed by PCR for 10 lines from each experiment (30 lines total). DNA was extracted using the cetyltrimethylammonium bromide (CTAB) protocol described in Li *et al.* (2020). Primers were designed to amplify a 611 bp fragment spanning the *Ef1α* promoter and *hpt* coding sequence (CDS) (MidEF1aF: 5′ TGCTGGGGTTTCTGGGGTTTGCATG 3′; MidHYGR: 5′ GCCAGTGATACACATGGGGATCAG 3′). The GoTaq Master Mix (M7132, Promega) was used with a reaction mix consisting of 1 µl diluted gDNA (1:10), 0.5 µl each primer, 6 µl 2× Master Mix and 3 µl H_2O, for a final volume of 11 µl. A negative control was included, where 1 µl H_2O was used in place of gDNA. The PCR conditions were as follows: 95 °C for 2 min, 30 cycles of 95 °C for 30 s, 59 °C for 30 s and 72 °C for 75 s, and finally 72 °C for 5 min.

Transgene confirmation by Illumina sequencing

A total of 12 stable lines (four per experiment) were shotgun sequenced to infer transgene copy number. *Anthoceros agrestis* thallus tissue was flash-frozen with liquid nitrogen and ground to a fine powder using a mortar and pestle. Illumina library preparation and paired-end sequencing (150 bp), with 50× coverage, was performed by Novogene Corp. Read trimming and quality check were done using fastp v0.23.3 (Chen *et al.*, 2018). We estimated transgene copy number by calculating the median read depth ratio between the *35S* promoter:GFP sequence and single-copy genes in the genome. Using Benchmarking Universal Single-Copy Orthologs (BUSCO; v5.4.7) (Manni *et al.*, 2021), we selected 375 single-copy genes (Supplementary Table S1) from *A. agrestis* for read-depth comparison. BWA (v0.7.17) (Li and Durbin, 2009) and SAMtools (v1.17) (Danecek *et al.*, 2021) were used to map reads and calculate read depth, respectively, for the BUSCO genes and the transgene. The command lines and program parameters can be found on Figshare (http://doi.org/10.6084/m9.figshare.24243559).

Fig. 1. Biolistic method overview. Healthy *A. agrestis* thallus tissue, grown on AG medium containing 0.2% sucrose, is collected and homogenized. Tissue is washed, filtered, and placed in a 2.5 cm diameter circle onto AG medium containing 2% sucrose. The tissue was allowed to recover for 7 d both before and after transformation. The tissue is pooled from all replicates, homogenized again, and placed onto filter paper on AG medium containing 0.2% sucrose to recover for 3 d. For antibiotics selection, tissue is transferred to AG medium containing 0.2% sucrose and 10 mg l^{-1} hygromycin. Transformed thallus tissue is visible approximately 8–10 weeks after transformation.

Transgene confirmation by nanopore sequencing

To confirm transgene insertion, four stably transformed lines were selected for Oxford Nanopore long-read sequencing. We used two different sequencing approaches. The first one, which included lines A1 and B3, used real-time adaptive sequencing (Payne *et al.*, 2021) to enrich reads that mapped to the Aa049 construct. Genomic DNA libraries were separately constructed using the Ligation Sequencing Kit V14 (Oxford Nanopore Technologies, SQK-LSK114). The line A1 library was loaded onto a MinION flowcell (R10.4.1) first and sequenced until at least 1000 mapped reads were collected. The flowcell was then washed with nuclease using the EXP-WSH004 kit (Oxford Nanopore Technologies). The line B3 library was subsequently loaded and sequenced until pores were no longer available. The mapped reads were inspected in Geneious Prime 2023.2.1 (https://www.geneious.com) using a combination of BLAST and homology annotation to identify reads that aligned to both Aa049 and *A. agrestis* genome, and to determine the insertion sites. For the second approach, which included lines B1 and C2, no enrichment was attempted and the genomes were shotgun sequenced. Genomic DNA libraries were constructed using the Native Barcoding Kit (SQK-NBD114.24) and sequenced together on a MinION flowcell (R10.4.1). Contigs were assembled by Flye v2.9.3 (Kolmogorov *et al.*, 2019) and inspected in Geneious using a combination of BLAST and homology annotation to identify the transgene integration sites.

Transformation of additional hornwort species

To test the applicability of our method in other hornworts, we selected nine species spanning seven genera and all of the five hornwort families (*Anthoceros fusiformis*, *Anthoceros punctatus*, *Anthoceros tuberculatus*, *Leiosporoceros dussii*, *Megaceros flagellaris*, *Notothylas orbicularis*, *Phaeoceros* sp., *Phaeomegaceros chiloensis*, and *Phymatoceros phymatodes*). Cultures were maintained as described earlier. Transformation of these species followed the same method used for *A. agrestis*, using the Aa049 construct.

Fluorescent protein-tagging and transformation

The Rubisco small subunit (*RbcS*, AagrOXF_evm.model.utg000008l.255.1) and Rubisco activase (*RCA*, AagrOXF_evm.model.utg000011l.50.1) CDS were identified in the *A. agrestis* genome (Li *et al.*, 2020) using Orthofinder (v2.5.4) (Emms and Kelly, 2019). In the case of *RbcS*, multiple copies of the gene were present, and therefore a copy that showed consistently high expression across multiple conditions was selected to ensure that it was a functional isoform (Li *et al.*, 2020). DNA fragments were synthesized by Twist Biosciences and assembled into L1 vectors. *RCA*, tagged with the *mVenus* fluorescent protein was under the control of the *EF1α* promoter and *NoS* terminator ('RCA_L1'; Supplementary Fig. S1). *RbcS*, tagged with *mScarlet-I*, was under the control of the *A. agrestis RbcS* promoter and *NoS* terminator ('RbcS_L1'; Supplementary Fig. S1). The L1 construct was combined with the $Ef1\alpha_{pro}$:*hpt*:NoS_{ter} construct in the *pCSA* L2 vector ('pDJL3' and 'pDJL4'; Supplementary Fig. S1). Plasmid maps and sequences can be found on Figshare (http://doi.org/10.6084/m9.figshare.24243559) and in Supplementary Fig. S1. *Anthoceros agrestis* transient and stable transformation followed the method described earlier. For transient transformation, the L1 constructs of *RCA-mVenus* (RCA_L1) and *RbcS-mScarlet-I* (RbcS_L1) were co-transformed at a ratio of 1:1. For stable transformation, the L2 constructs of *RCA-mVenus* (pDJL4) and

RbcS-mScarlet-I (pDJL3), each carrying a selectable marker, were transformed separately.

Results

Efficient transient biolistic transformation

Experiments were conducted to refine the biolistic method for *A. agrestis*, including varying shooting distance, gold microparticle size, DNA precipitation methods and hornwort tissue growth conditions (Supplementary Fig. S2). It was determined that the optimal method parameters encompassed the use of 1 μm gold particles, a helium pressure of 600 psi, a vacuum pressure of 711 mmHg, a bombardment plate distance of 14 cm from the source, 20 μg plasmid DNA, and a spermidine/$CaCl_2$ DNA precipitation, with hornwort thallus tissue grown on 2% sucrose AG medium for 7 d. These parameters were chosen for future experiments because more severe tissue damage was observed when bombarding at higher pressures and shorter plate distances, while a shorter recovery time post tissue homogenization and the polyethylene glycol/$MgCl_2$ precipitation method had lower transient transformation efficiency. The Aa049 construct was used in transformations to visualize transformation efficiency. This construct consisted of *GFP* fused to *Lti6b*, under the control of a *35S* promoter, to localize the GFP signal to the plasma membrane (Kurup *et al.*, 2005) and *hpt*, under the control of the native *Ef1α* promoter, for selection with hygromycin (Supplementary Fig. S1). To quantify the number of cells transiently expressing GFP, we developed an efficient semi-automatic procedure using CellProfiler (Stirling *et al.*, 2021). This method has previously been used to quantify the transient transformation efficiency in biolistically transformed onion and *Nicotiana benthamiana* (Miller *et al.*, 2021). We confirmed the results from CellProfiler with manual counting and found a strong linear correlation, with a Pearson correlation coefficient (*r*) of 0.98 (Supplementary Fig. S3). An empty vector control had an average of seven objects as GFP expressing cells, which was due to artifacts picked up by the stereoscope (Fig. 2).

Five separate experiments (with 10 replicates each) were performed to assess the efficacy and reproducibility of transient transformation (Fig. 2C). Results were quantified 48–72 h after transformation, with fluorescence first observed within 48 h. We found high variability between replicates in each experiment. For example, in experiment 3, one replicate had 1158 transiently expressing cells while another had 114. In addition, not all replicates were successfully transformed (i.e. no GFP signal observed from any cell). These were removed from downstream analysis (two to four per experiment; Fig. 2). It is unknown what caused inconsistencies, with potential factors being poor tissue health, tissue moisture level, or aggregation of gold particles on the macrocarrier, all of which can reduce transformation efficiency (Southgate *et al.*, 1995). Across all successfully transformed replicates, there was an average of 569 (±268) transiently expressing GFP cells from one bombardment experiment. The variability was reduced when comparing the means from each experiment, which ranged from 474 to 701 transient events (Fig. 2).

Recovery of stable transformants

Although transient transformation resulted in hundreds of events, it was initially challenging to recover stably transformed lines. In our earlier attempts, we allowed the bombarded tissue to recover for 7 d before cutting into 2 mm^2 pieces and transferring to AG medium containing 0.2% sucrose and 10 mg l^{-1} hygromycin. Over the following weeks, we observed that GFP-expressing tissue persisted; however, the surrounding tissue also survived much longer than other non-transformed tissue (Supplementary Fig. S4). HPT inactivates hygromycin via phosphorylation (Rao *et al.*, 1983) and in Arabidopsis HPT was shown to be secreted into the extracellular space (Zhang *et al.*, 2011). It is possible that hygromycin is inactivated in the medium surrounding transformed tissue, allowing untransformed tissue to survive and compete with the transformed tissue during regeneration. To overcome this, tissue was homogenized before being placed on selection medium to reduce the amount of non-transformed tissue surrounding the transformed tissue. After 8–10 weeks of selection the first regenerating hygromycin-resistant thallus tissue was visible and was transferred to freshly prepared selection medium for propagation (Fig. 1). This method was repeated across three separate experiments, with five replicates in experiments A and B, and four replicates in experiment C. These experiments regenerated 20, 49, and 12 individual lines, respectively, totaling 81 lines. The presence of the transgene was confirmed via fluorescence microscopy, where GFP was observed in thallus tissue (Fig 3A) and was localized to the plasma membrane (Fig. 3B), and PCR, with primers designed to span the *Ef1α* promoter and *hpt* CDS (Supplementary Figs S5–S7). On average, each bombardment of 0.2 g of tissue yielded six stable transformants.

A drawback of biolistic-mediated transformation is the potential for high transgene copy number, which may lead to instability and potential gene silencing (Kohli *et al.*, 2003). To assess the transgene copy number, we shotgun-sequenced four stable lines per experiment, and compared the median read depth of the *35Spro:GFP* sequence with the median read depth for a set of single-copy genes (here the BUSCO genes were used; Table 1; Supplementary Table S1). The whole plasmid was not used for read depth comparison as it contained the native hornwort *Ef1a* promoter and multiple copies of the *NoS* terminator. We found that 50% of the sequenced lines had a copy number fewer than four, and 30% had a single copy. Several lines had very large copy numbers, with the highest estimated at 75.

Currently, for the *A. agrestis* Oxford strain we lack the capability to stimulate the formation of sexual structures *in vitro*, thus impeding our ability to observe the inheritance pattern of transgenes in subsequent generations. To confirm transgene integration into the genome, we selected lines A1, B1, B3, and

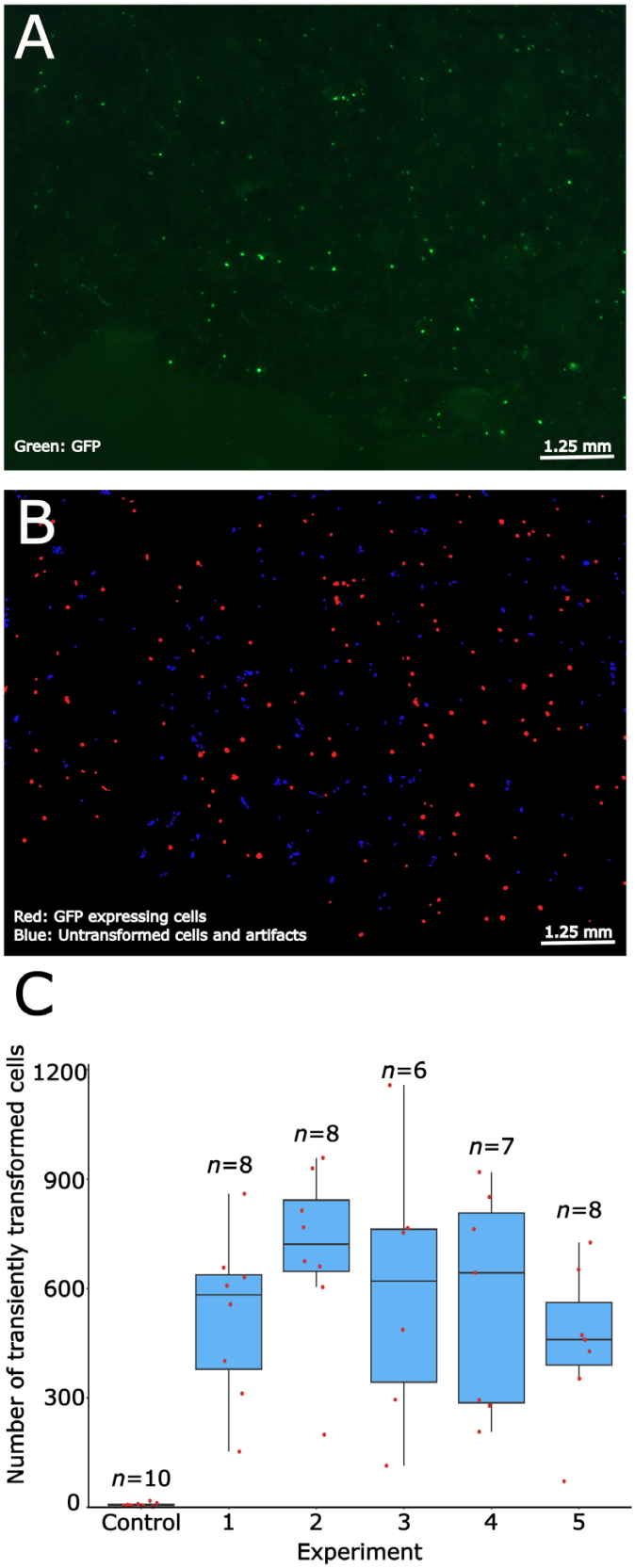

Fig. 2. Transient transformation of *Anthoceros agrestis* and event quantification. (A) The unprocessed image of tissue transiently expressing plasma membrane-localized green fluorescent protein (GFP), taken with a Leica M205 stereomicroscope. (B) The same image in (A) after processing with CellProfiler, where blue signals represent artifact objects or cells/tissue not expressing GFP and red signals are transformed cells expressing GFP. (C) Boxplot displaying the number of cells transiently expressing GFP, across five separate experiments and an empty vector control. Individual replicates are plotted as red dots. The box represents the 25th and 75th percentile, with the horizontal line being the median value and the vertical lines marking the minimum and maximum, excluding outliers.

C2 for Oxford Nanopore long-read sequencing. We were able to identify reads and contigs that spanned both the Aa049 and *A. agrestis* genomic region, allowing us to pinpoint the insertion sites (Supplementary Table S2). The only exception is line B1, for which we were unable to obtain sufficient sequence.

Applicability to other hornwort species

To assess the applicability of the biolistic method to other hornwort species, we tested a total of nine species spanning the entire hornwort phylogeny: *Anthoceros fusiformis*, *Anthoceros punctatus*, *Anthoceros tuberculatus*, *Leiosporoceros dussii*, *Megaceros flagellaris*, *Notothylas orbicularis*, *Phaeoceros* sp., *Phaeomegaceros chiloensis*, and *Phymatoceros phymatodes*. The majority of species had fewer transiently expressing GFP cells than *A. agrestis*, while both *A. punctatus* and *N. orbicularis* had a greater number (Fig. 4; Supplementary Fig. S8). Stable transformants were obtained for *A. fusiformis* with 29 lines recovered from one experiment (Fig. 5; Supplementary Fig. S9). Recovery of stable transformants was attempted for the remaining species although this was unsuccessful. These results indicate that the method needs to be optimized for each species in order to increase the efficiency of transient transformation and to obtain stable transformants.

Transient and stable expression of fluorescently tagged Rubisco and Rubisco activase

To demonstrate the applicability of the biolistics-mediated transformation method for hornwort studies, we investigated the structure of hornwort pyrenoids by localizing two putative pyrenoid-localized proteins, Rubisco activase (RCA) and the Rubisco Small subunit (RbcS), through co-transformation of *A. agrestis*. In separate vectors, the *RCA* CDS was fused to the *mVenus* CDS and the *RbcS* CDS was fused to the *mScarlet-I* CDS (Supplementary Fig. S1). Co-transformation of these two constructs, at a ratio of 1:1, clearly showed that RCA and RbcS co-localized, with fluorescence tightly confined within round structures in the chloroplast corresponding to pyrenoids (Fig. 6). Pyrenoids appear as distinct black holes under the chlorophyll autofluorescence channel, which is consistent with the early ultrastructural studies based on transmission electron microscopy (Vaughn *et al.*, 1992). Furthermore, we obtained stably transformed lines expressing either the RCA:mVenus or the RbcS:mScarlet-I constructs. A total of 28 and 3 lines were regenerated for the RCA:mVenus and the RbcS:mScarlet-I constructs, respectively. Again, the fluorescence signals were

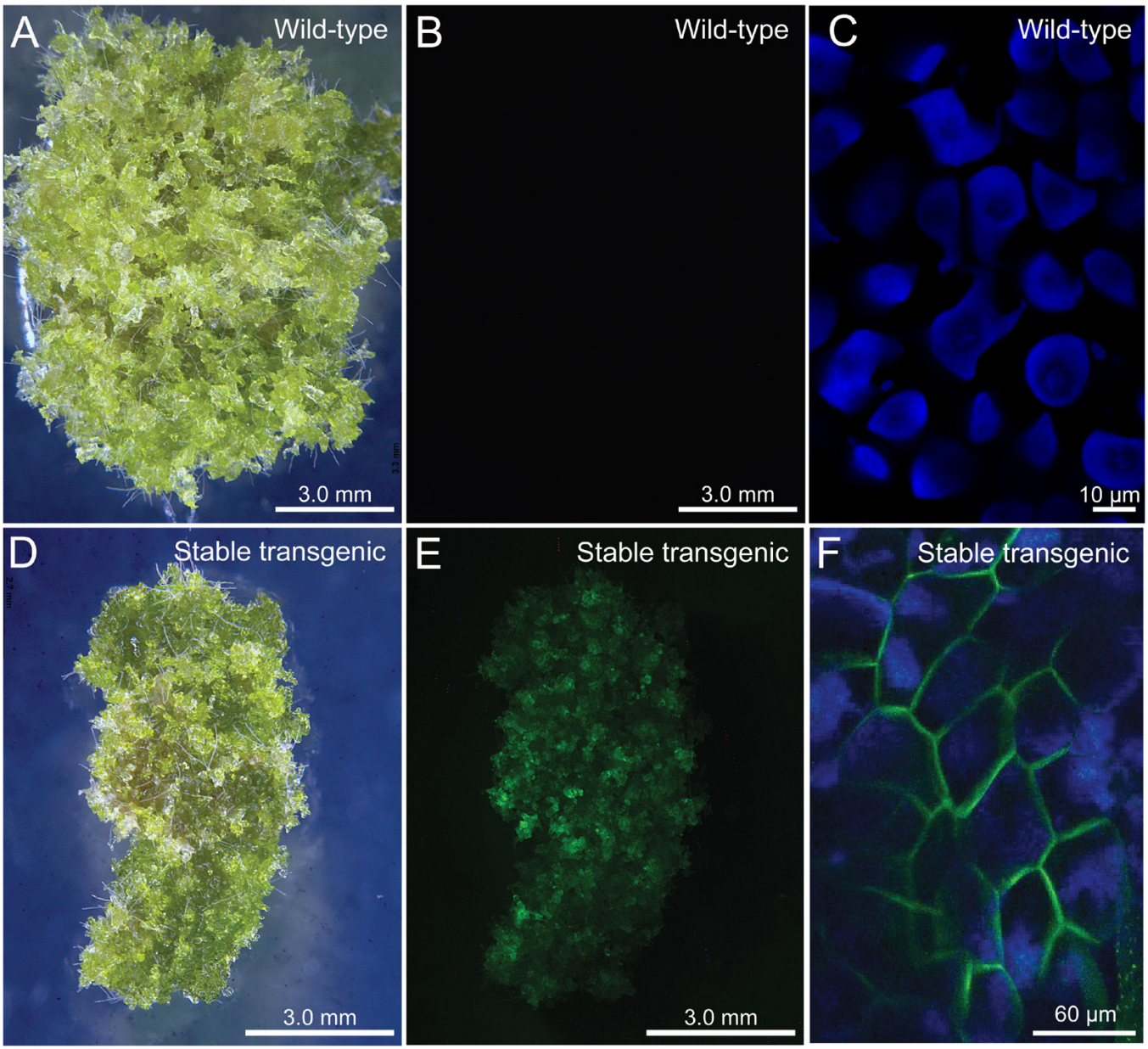

Fig. 3. Stable transformants of *Anthoceros agrestis* expressing membrane-localized green fluorescent protein (GFP). Wild-type (A–C) and transformed (D–F) thallus tissue was imaged using a Leica M205 stereomicroscope, with the light (A, D) and GFP (B, E) channels, and a Leica TCS SP5 laser scanning confocal microscope (C, F), displaying chlorophyll autofluorescence in blue and GFP signal in green.

highly concentrated in pyrenoid structures that are devoid of chlorophyll autofluorescence.

Discussion

A biolistic method for transient and stable transformation across the hornwort phylogeny

Our new method resulted in a high number of transient and stable events for *A. agrestis*. From 0.2 g of bombarded tissue, we obtained on average 569 (±268) transiently transformed cells and six stable insertion lines. Furthermore, we provide the first account of transient transformation in *A. tuberculatus*, *M. flagellaris*, *N. orbicularis*, *Phaeoceros* sp., *Phaeomegaceros chiloensis*, and *Phymatoceros phymatodes*, together covering all the hornwort families. It is important to note that these species are deeply diverged; they share the most recent common ancestor almost 300 million years ago (Bechteler *et al.*, 2023), which predates the origin of flowering plants (Ramírez-Barahona *et al.*, 2020). Successful transient transformation of multiple hornwort species suggests that our method is widely applicable across taxa, thus broadening the scope of genetic manipulation in

Table 1. Transgene copy number estimate for the sequenced stable lines

	Line	BUSCO median read depth	GFP cassette median Read Depth	BUSCO–GFP ratio	Inferred copy number
Experiment A	A1	53	370	6.98	7
	A2	41	552	13.46	13
	A3	53	1552	29.28	29
	A4	42	23	0.55	1
Experiment B	B1	50	50	1.00	1
	B2	67	133	1.99	2
	B3	58	45	0.78	1
	B4	74	5541	74.88	75
Experiment C	C1	48	153	3.19	3
	C2	44	45	1.02	1
	C3	28	1826	65.21	65
	C4	42	422	10.05	10

Note that although two lines had a BUSCO–GFP ratio of less than 1, GFP expression was still observed and there was even read coverage across the entire GFP cassette with no missing sequences. BUSCO, Benchmarking Universal Single-Copy Orthologue; GFP, green fluorescent protein.

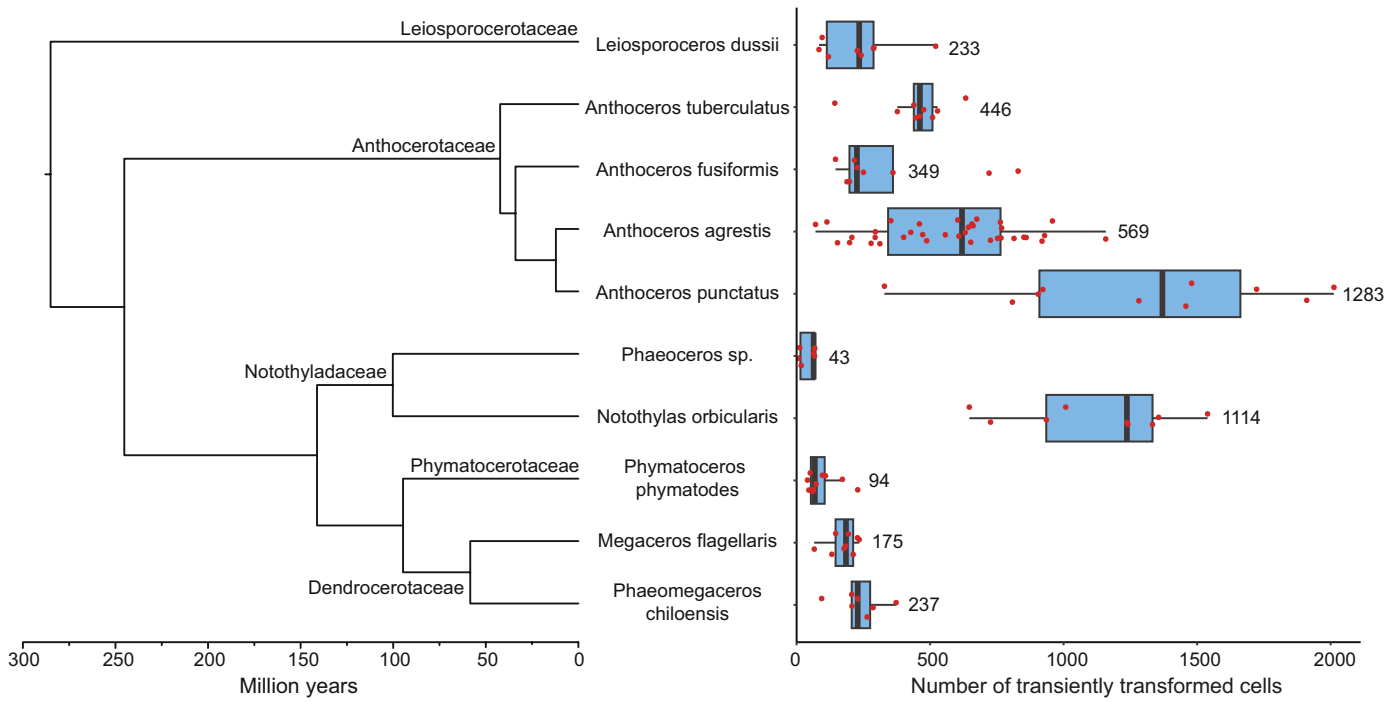

Fig. 4. Transient transformation of hornwort species across the phylogeny. Our method can be directly applied to generate transient transformants in species covering all hornwort families and most of the genera. Phylogenetic tree displays timing of divergence, adapted from Bechteler *et al.* (2023). Red dots represent the value of replicates and numbers represent the average number of transiently transformed cells per bombardment. The box represents the 25th and 75th percentile, with the vertical line being the median value. The horizontal lines represent the minimum and maximum, excluding outliers.

hornworts. The ability to transform diverse hornwort species enables comparative studies to identify conserved genetic elements, especially for convergently evolved traits. For example, pyrenoids have originated independently approximately five to six times during hornwort evolution, resulting in vastly different morphologies and CCM strength across species (Vaughn *et al.*, 1990; Hanson *et al.*, 2002; Villarreal and Renner, 2012; Li *et al.*, 2017). Understanding the genetic basis of such repeated evolution could have important implications in engineering CCMs in other plant species. Likewise, U/V sex chromosomes have experienced multiple gains and losses in hornworts (Villarreal and Renner, 2013). Future work could use our biolistics method to test if similar genetic elements have been convergently recruited to sex chromosomes.

Despite the relatively high number of transient events, we had mixed success in generating stable transformants from diverse hornwort species. While 29 *A. fusiformis* stable lines were recovered from one experiment (Fig. 5), we did not recover

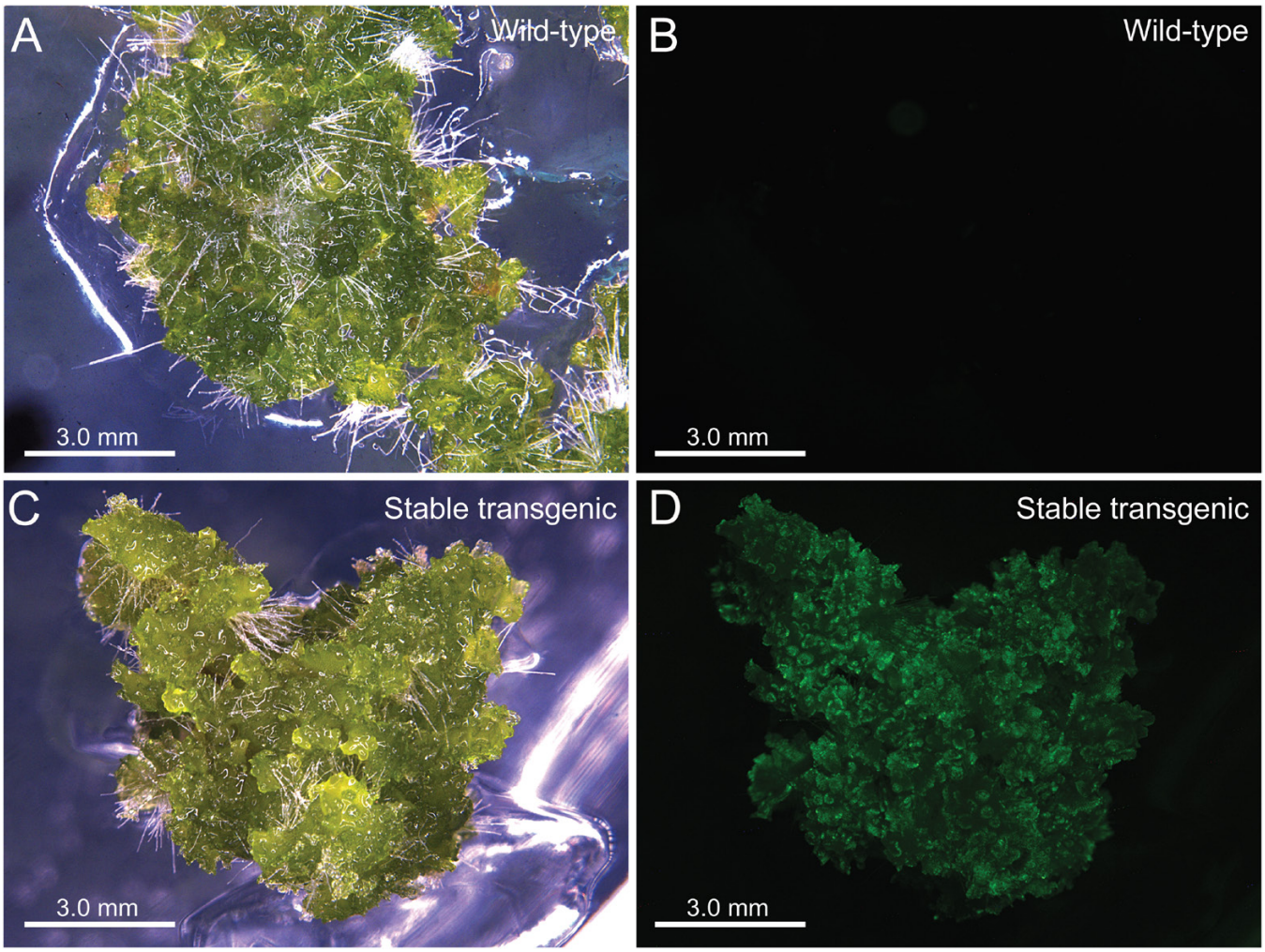

Fig. 5. Stable transformants of *Anthoceros fusiformis* express membrane localized green fluorescent protein (GFP). Wild-type (A, B) and stably transformed (C, D) thallus tissue was imaged using a Leica M205 stereomicroscope, with the light (A, C) and GFP (B, D) channels.

stable events from the remaining species. It is likely that the method needs to be optimized for each species. In particular, we have observed that a number of species have a slower growth rate on AG medium, which indicates that the post-homogenization recovery time may need to be extended. In our constructs, the *A. agrestis Ef1α* promoter drives *hpt* expression; however, it is possible that this promoter may not function well in other hornwort species, especially considering the timing of divergence (Fig. 4), and their native *Ef1a* promoter is required. The optimal antibiotic concentration to select for transgenic events may also vary between species.

Relative high frequency of low transgene copy number in stably transformed lines

A common issue for biolistic-mediated transformation is the possibility of multiple transgene insertions into the genome. Here we report that 33% of sequenced transgenic lines were estimated to have single-copy insertions, and 50% of the lines have fewer than four copies. The frequency of low-copy insertions is much higher when compared with biolistic transformation of other bryophytes. Studies in the liverwort *Marchantia polymorpha* and the moss *Physcomitrium patens* found that only 10% of regenerated lines had single copies of the transgene (Irifune *et al.*, 1996; Šmídková *et al.*, 2010). Nevertheless, we did occasionally observe lines with a large transgene copy number, with two lines having an estimated 63 and 73 copies, respectively. While *Agrobacterium*-mediated transformation of hornworts has been demonstrated, the frequency of low copy number events was not reported (Frangedakis *et al.*, 2021b; Waller *et al.*, 2023). It is likely that the frequency of single-copy insertions can be further increased using a minimal cassette, where the genes of interest are amplified using PCR, eliminating the backbone from transformation. This technique typically requires less DNA for transformation. Two studies in wheat aimed to increase the number of single copy events by

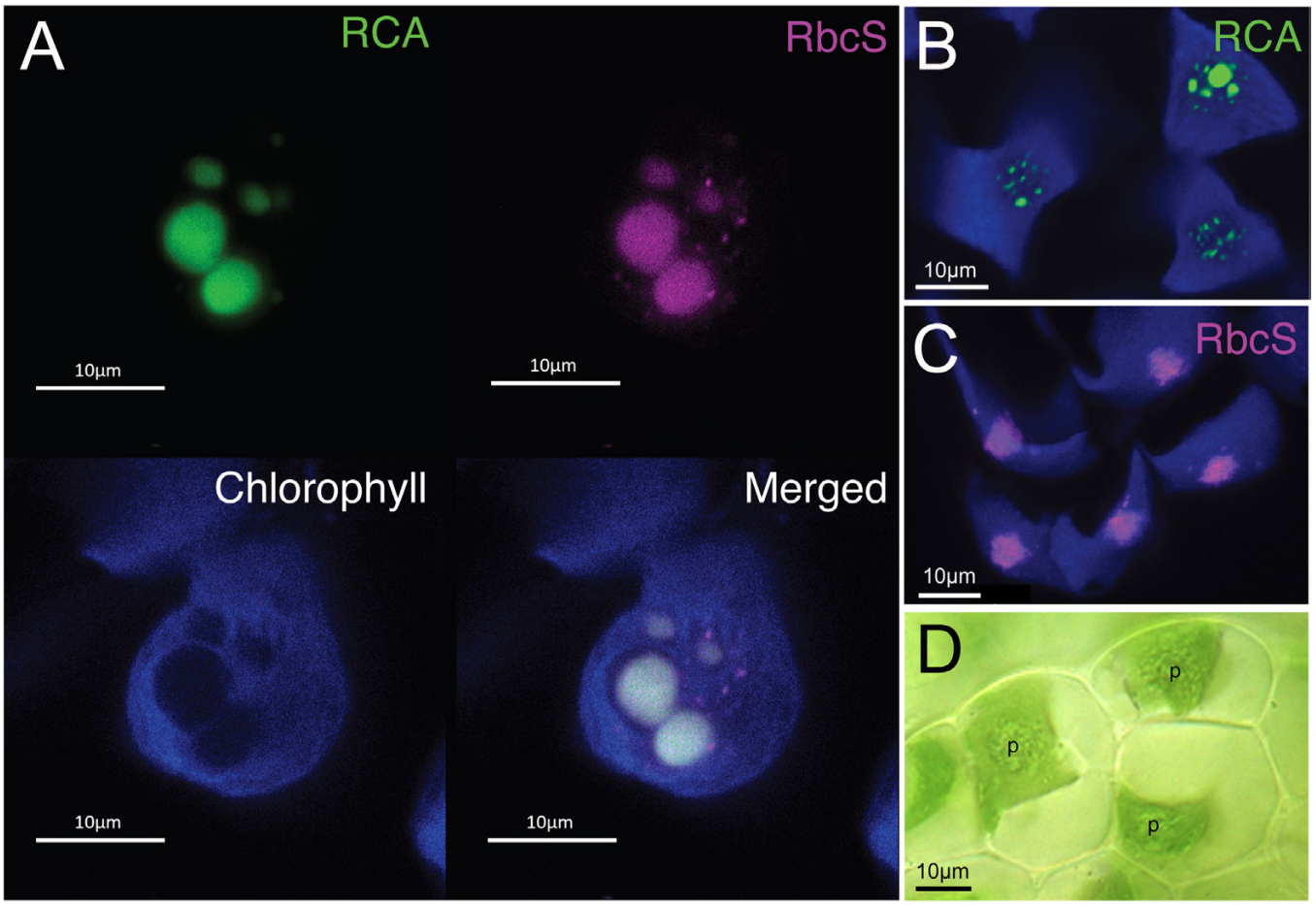

Fig. 6. Transient and stable transformation of pyrenoid-related genes in *Anthoceros agrestis*. (A) *Anthoceros agrestis* thallus tissue was transiently co-transformed with *RCA:mVenus* and *RbcS:mScarlet-I* constructs. The pyrenoid regions are packed with tagged RCA (green) and RbcS (magenta) and lack chlorophyll autofluorescence (blue). The overlapping mScarlet-I and mVenus fluorescence signal strongly suggests co-localization of RbcS and RCA to pyrenoids. (B, C) *Anthoceros agrestis* was stably transformed with either *RCA:mVenus* (B) or *RbcS:mScarlet-I* (C). Thallus tissue expressing the given constructs was captured using a Leica TCS SP5 laser scanning confocal microscope, with chlorophyll in blue. (D) Transmission light microscopy image of *A. agrestis* chloroplasts with pyrenoids (p).

using minimal cassettes, resulting in an average of 38% and 50% of single-copy insertions (Tassy *et al.*, 2014; Ismagul *et al.*, 2018), while in rice 80% of regenerated lines were estimated to have fewer than two transgene copies (Fu *et al.*, 2000).

Using fluorescent protein tagging to visualize hornwort pyrenoids

Application of this method enabled us to observe localization of fluorescently tagged proteins within 48–72 h post-bombardment and 9 d from the point the tissue was first homogenized. The biolistic method thus provides the ability to quickly assess protein function, localization, and interactions without the need to generate stable transformants. We demonstrated that our method can be used to study proteins associated with pyrenoids and CCM function.

Pyrenoids are micro-compartments within the chloroplasts of algae and hornworts that are composed predominantly of Rubisco. This aggregation of Rubisco enables the function of a biophysical CCM providing a central locus in which to concentrate CO_2. While pyrenoids are present in many algal species and have been extensively studied in the model alga *Chlamydomonas reinhardtii* (He *et al.*, 2023), hornworts are the only land plants with pyrenoids and have received little research attention (Li *et al.*, 2017). Early ultrastructural studies reported that hornwort pyrenoids are tightly sandwiched by thylakoids (as opposed to starch sheaths in algae) (Burr, 1970; Vaughn *et al.*, 1992), and based on immunogold labeling are indeed the locations where Rubisco is concentrated (Vaughn *et al.*, 1990). We set out to visualize pyrenoids by fluorescent protein tagging and to establish pyrenoid marker proteins for future studies. To this end, we focused on the Rubisco small subunit (RbcS) as well as Rubisco activase (RCA), which is required for Rubisco activation and activity maintenance (McKay *et al.*, 1991). In *C. reinhardtii* both proteins are known to localize predominantly in pyrenoids (Mackinder *et al.*, 2017). We co-transformed

constructs harboring the RCA and RbcS CDSs tagged with the mVenus and mScarlet-I fluorescent protein, respectively, into *A. agrestis* thalli. RCA and RbcS were found to clearly co-localize to pyrenoids based on the overlapping mVenus and mScarlet-I signals (Fig. 6). Importantly, it is now possible to use either fluorescently tagged RbcS or RCA as a pyrenoid marker, and co-transform it with candidate genes to build a spatial protein localization model for hornwort CCMs. Furthermore, we show the successful regeneration of lines stably expressing either *RbcS:mScarlet-I* or *RCA:mVenus*. Currently, these transformants are being used to track pyrenoid development and to understand how it is impacted by environmental factors such as CO_2 concentration.

In conclusion, we report the first biolistic protocol for transformation of a phylodiverse set of hornwort species, as well as the first protein localization study in the model hornwort *Anthoceros agrestis*. We expect that our work will allow new avenues for investigation and biotechnological applications, such as genome editing. The achievement of both stable and transient transformation provides powerful tools for studying gene function in hornworts. These advances lay the foundation for future research aimed at unraveling the mysteries of hornwort biology and harnessing their unique characteristics for sustainable agriculture.

Supplementary data

The following supplementary data are available at *JXB* online.

Fig. S1. Plasmid maps used for transformations.

Fig. S2. Preliminary assessments of different parameters for optimizing biolistics-mediated transformation method.

Fig. S3. Correlation between manual and CellProfiler counting of cells transiently expressing GFP.

Fig. S4. Transformed *A. agrestis* tissue on hygromycin selection.

Fig. S5. *Anthoceros agrestis* stable lines regenerated from experiment A.

Fig. S6. *Anthoceros agrestis* stable lines regenerated from experiment B.

Fig. S7. *Anthoceros agrestis* stable lines regenerated from experiment C.

Fig. S8. Representative photos of hornwort species used for CellProfiler quantification.

Fig. S9. *Anthoceros fusiformis* stable lines.

Table S1. BUSCO genes used in transgene copy number estimation analysis.

Table S2. Transgene insertion sites.

Acknowledgements

We thank Eftychis Frangedakis for providing the materials in the OpenPlant toolkit and transformation advice, Mamta Srivastava for helping with confocal and fluorescence microscopy, Jenna Sins and Evan Smith for laboratory assistance, and the Editor and two anonymous reviewers for their comments that substantially improved this manuscript.

Author contributions

FWL and JVE: conceptualization; DL: formal analysis; FWL, JVE, and LHG: funding acquisition; DL, TAR, AG, and PWS: investigation; DL and AG: methodology; FWL, JVE, and LHG: supervision; DL and TAR: visualization; DL and FWL: writing—original draft.

Conflict of interest

The authors declare they have no conflicts of interest.

Funding

This work was funded by NSF IOS 1923011 to FWL and JVE, and NSF MCB 2213841 to FWL and LHG.

Data availability

The raw Illumina reads for quantifying transgene copy numbers are available in the NCBI SRA (under BioProject PRJNA1029596). The detailed protocol is also available at protocol.io (DOI: dx.doi.org/10.17504/protocols.io.3byl49792go5/v1).

References

Adler L, Díaz-Ramos A, Mao Y, Pukacz KR, Fei C, McCormick AJ. 2022. New horizons for building pyrenoid-based CO_2-concentrating mechanisms in plants to improve yields. Plant Physiology **190**, 1609–1627.

Atkinson N, Mao Y, Chan KX, McCormick AJ. 2020. Condensation of Rubisco into a proto-pyrenoid in higher plant chloroplasts. Nature Communications **11**, 6303.

Bechteler J, Gabriel Peñaloza-Bojacá G, Bell D, *et al*. 2023. Comprehensive phylogenomic time tree of bryophytes reveals deep relationships and uncovers gene incongruences in the last 500 million years of diversification. American Journal of Botany **110**, e16249.

Boynton JE, Gillham NW, Harris EH, *et al*. 1988. Chloroplast transformation in *Chlamydomonas* with high velocity microprojectiles. Science **240**, 1534–1538.

Burr FA. 1970. Phylogenetic transitions in the chloroplasts of the Anthocerotales. I. The number and ultrastructure of the mature plastids. American Journal of Botany **57**, 97–110.

Chatterjee P, Schafran P, Li F-W, Meeks JC. 2022. *Nostoc* talks back: Temporal patterns of differential gene expression during establishment of *Anthoceros-Nostoc* symbiosis. Molecular Plant-Microbe Interactions **35**, 917–932.

Chen S, Zhou Y, Chen Y, Gu J. 2018. fastp: an ultra-fast all-in-one FASTQ preprocessor. Bioinformatics **34**, i884–i890.

Danecek P, Bonfield JK, Liddle J, *et al*. 2021. Twelve years of SAMtools and BCFtools. GigaScience **10**, giab008.

Emms DM, Kelly S. 2019. OrthoFinder: phylogenetic orthology inference for comparative genomics. Genome Biology **20**, 238.

Frangedakis E, Shimamura M, Villarreal JC, Li F-W, Tomaselli M, Waller M, Sakakibara K, Renzaglia KS, Szövényi P. 2021a. The hornworts: morphology, evolution and development. New Phytologist **229**, 735–754.

Frangedakis E, Waller M, Nishiyama T, *et al*. 2021b. An *Agrobacterium*-mediated stable transformation technique for the hornwort model *Anthoceros agrestis*. New Phytologist **232**, 1488–1505.

Fu X, Duc LT, Fontana S, Bong BB, Tinjuangjun P, Sudhakar D, Twyman RM, Christou P, Kohli A. 2000. Linear transgene constructs lacking vector backbone sequences generate low-copy-number transgenic plants with simple integration patterns. Transgenic Research **9**, 11–19.

Gunadi A, Li F-W, Van Eck J. 2022. Accelerating gametophytic growth in the model hornwort *Anthoceros agrestis*. Applications in Plant Sciences **10**, e11460.

Hanson D, Andrews TJ, Badger MR. 2002. Variability of the pyrenoid-based CO_2 concentrating mechanism in hornworts (Anthocerotophyta). Functional Plant Biology **29**, 407–416.

Hatcher R. 1965. Towards the establishment of a pure culture collection of Hepaticae. Bryologist **68**, 227–231.

He S, Crans VL, Jonikas MC. 2023. The pyrenoid: the eukaryotic CO_2-concentrating organelle. The Plant Cell **35**, 3236–3259.

Irifune K, Ono K, Takahashi M, Murakami H, Morikawa H. 1996. Stable transformation of cultured cells of the liverwort *Marchantia polymorpha* by particle bombardment. Transgenic Research **5**, 337–341.

Ismagul A, Yang N, Maltseva E, *et al*. 2018. A biolistic method for high-throughput production of transgenic wheat plants with single gene insertions. BMC Plant Biology **18**, 135.

Kohli A, Twyman RM, Abranches R, Wegel E, Stoger E, Christou P. 2003. Transgene integration, organization and interaction in plants. Plant Molecular Biology **52**, 247–258.

Kolmogorov M, Yuan J, Lin Y, Pevzner PA. 2019. Assembly of long, error-prone reads using repeat graphs. Nature Biotechnology **37**, 540–546.

Kurup S, Runions J, Köhler U, Laplaze L, Hodge S, Haseloff J. 2005. Marking cell lineages in living tissues. The Plant Journal **42**, 444–453.

Lacroix B, Citovsky V. 2020. Biolistic approach for transient gene expression studies in plants. Methods in Molecular Biology **2124**, 125–139.

Li F-W, Nishiyama T, Waller M, *et al*. 2020. *Anthoceros* genomes illuminate the origin of land plants and the unique biology of hornworts. Nature Plants **6**, 259–272.

Li F-W, Villarreal JC, Szövényi P. 2017. Hornworts: An overlooked window into carbon-concentrating mechanisms. Trends in Plant Science **22**, 275–277.

Li H, Durbin R. 2009. Fast and accurate short read alignment with Burrows–Wheeler transform. Bioinformatics **25**, 1754–1760.

Mackinder LCM, Chen C, Leib RD, Patena W, Blum SR, Rodman M, Ramundo S, Adams CM, Jonikas MC. 2017. A spatial interactome reveals the protein organization of the algal CO_2-concentrating mechanism. Cell **171**, 133–147.e14.

Manni M, Berkeley MR, Seppey M, Simão FA, Zdobnov EM. 2021. BUSCO update: Novel and streamlined workflows along with broader and deeper phylogenetic coverage for scoring of eukaryotic, prokaryotic, and viral genomes. Molecular Biology and Evolution **38**, 4647–4654.

Martin-Ortigosa S, Wang K. 2014. Proteolistics: a biolistic method for intracellular delivery of proteins. Transgenic Research **23**, 743–756.

McKay RML, Gibbs SP, Vaughn KC. 1991. RuBisCo activase is present in the pyrenoid of green algae. Protoplasma **162**, 38–45.

Meeks JC. 1998. Symbiosis between nitrogen-fixing cyanobacteria and plants. Bioscience **48**, 266–276.

Meyer MT, McCormick AJ, Griffiths H. 2016. Will an algal CO_2-concentrating mechanism work in higher plants? Current Opinion in Plant Biology **31**, 181–188.

Miller K, Eggenberger AL, Lee K, Liu F, Kang M, Drent M, Ruba A, Kirscht T, Wang K, Jiang S. 2021. An improved biolistic delivery and analysis method for evaluation of DNA and CRISPR-Cas delivery efficacy in plant tissue. Scientific Reports **11**, 7695.

Morris JL, Puttick MN, Clark JW, Edwards D, Kenrick P, Pressel S, Wellman CH, Yang Z, Schneider H, Donoghue PCJ. 2018. The timescale of early land plant evolution. Proceedings of the National Academy of Sciences, USA **115**, E2274–E2283.

Nelson JM, Hauser DA, Li F-W. 2021. The diversity and community structure of symbiotic cyanobacteria in hornworts inferred from long-read amplicon sequencing. American Journal of Botany **108**, 1731–1744.

Neubauer A, Ruaud S, Waller M, Frangedakis E, Li F-W, Nötzold SI, Wicke S, Bailly A, Szövényi P. 2022. Step-by-step protocol for the isolation and transient transformation of hornwort protoplasts. Applications in Plant Sciences **10**, e11456.

Payne A, Holmes N, Clarke T, Munro R, Debebe BJ, Loose M. 2021. Readfish enables targeted nanopore sequencing of gigabase-sized genomes. Nature Biotechnology **39**, 442–450.

Ramírez-Barahona S, Sauquet H, Magallón S. 2020. The delayed and geographically heterogeneous diversification of flowering plant families. Nature Ecology and Evolution **4**, 1232–1238.

Rao RN, Allen NE, Hobbs JN Jr, Alborn WE Jr, Kirst HA, Paschal JW. 1983. Genetic and enzymatic basis of hygromycin B resistance in *Escherichia coli*. Antimicrobial Agents and Chemotherapy **24**, 689–695.

Sanford JC, Klein TM, Wolf ED, Allen N. 1987. Delivery of substances into cells and tissues using a particle bombardment process. Particulate Science and Technology **5**, 27–37.

Sauret-Güeto S, Frangedakis E, Silvestri L, Rebmann M, Tomaselli M, Markel K, Delmans M, West A, Patron NJ, Haseloff J. 2020. Systematic tools for reprogramming plant gene expression in a simple model, *Marchantia polymorpha*. ACS Synthetic Biology **9**, 864–882.

Šmídková M, Holá M, Angelis KJ. 2010. Efficient biolistic transformation of the moss *Physcomitrella patens*. Biologia Plantarum **54**, 777–780.

Southgate EM, Davey MR, Power JB, Marchant R. 1995. Factors affecting the genetic engineering of plants by microprojectile bombardment. Biotechnology Advances **13**, 631–651.

Stirling DR, Swain-Bowden MJ, Lucas AM, Carpenter AE, Cimini BA, Goodman A. 2021. CellProfiler 4: improvements in speed, utility and usability. BMC Bioinformatics **22**, 433.

Svab Z, Maliga PAL. 1993. High-frequency plastid transformation in tobacco by selection for a chimeric aadA gene. Proceedings of the National Academy of Sciences, USA **90**, 913–917.

Svitashev S, Schwartz C, Lenderts B, Young JK, Mark Cigan A. 2016. Genome editing in maize directed by CRISPR–Cas9 ribonucleoprotein complexes. Nature Communications **7**, 13274.

Szövényi P, Frangedakis E, Ricca M, Quandt D, Wicke S, Langdale JA. 2015. Establishment of *Anthoceros agrestis* as a model species for studying the biology of hornworts. BMC Plant Biology **15**, 98.

Tassy C, Partier A, Beckert M, Feuillet C, Barret P. 2014. Biolistic transformation of wheat: increased production of plants with simple insertions and heritable transgene expression. Plant Cell, Tissue and Organ Culture **119**, 171–181.

Vaughn KC, Campbell EO, Hasegawa J, Owen HA, Renzaglia KS. 1990. The pyrenoid is the site of ribulose 1,5-bisphosphate carboxylase/oxygenase accumulation in the hornwort (Bryophyta: Anthocerotae) chloroplast. Protoplasma **156**, 117–129.

Vaughn KC, Ligrone R, Owen HA, Hasegawa J, Campbell EO, Renzaglia KS, Monge-Najera J. 1992. The anthocerote chloroplast: a review. New Phytologist **120**, 169–190.

Villarreal JC, Renner SS. 2012. Hornwort pyrenoids, carbon-concentrating structures, evolved and were lost at least five times during the last 100 million years. Proceedings of the National Academy of Sciences, USA **109**, 18873–18878.

Villarreal JC, Renner SS. 2013. Correlates of monoicy and dioicy in hornworts, the apparent sister group to vascular plants. BMC Evolutionary Biology **13**, 239.

Waller M, Frangedakis E, Marron AO, Sauret-Gueto S, Rever J, Sabbagh CRR, Hibberd JM, Haseloff J, Renzaglia K, Szövényi P. 2023. An optimised transformation protocol for *Anthoceros agrestis* and three more hornwort species. The Plant Journal **114**, 699–718.

Zhang H, Zhang L, Gao B, Fan H, Jin J, Botella MA, Jiang L, Lin J. 2011. Golgi apparatus-localized synaptotagmin 2 is required for unconventional secretion in *Arabidopsis*. PLoS One **6**, e26477.

Zhang Y, Liang Z, Zong Y, Wang Y, Liu J, Chen K, Qiu J-L, Gao C. 2016. Efficient and transgene-free genome editing in wheat through transient expression of CRISPR/Cas9 DNA or RNA. Nature Communications **7**, 12617.